STUDIA UBB CHEMIA, LXV, 4, 2020 (p. 177-201)
(RECOMMENDED CITATION)
DOI:10.24193/subbchem.2020.4.14

ADSORPTION AND CORROSION INHIBITIVE PROPERTIES OF *ORYZA GLABERRIMA* HUSK EXTRACT ON ALUMINIUM IN H_2SO_4 SOLUTION: ISOTHERM, KINETIC AND THERMODYNAMIC STUDIES

LEKAN TAOFEEK POPOOLA[a*]

ABSTRACT. In this study, isotherm, kinetic and thermodynamic studies of corrosion inhibitory properties of *Oryza Glaberrima* husk extract (OGHE) on aluminium in 1.5 M H_2SO_4 solution was investigated via mass loss measurement. Aluminium coupon and OGHE were characterized using SEM, EDS, FTIR and AAS. Increase in Al corrosion rate in H_2SO_4 solution was observed as exposure period (24 - 120 hrs) and temperature (293 - 333K) were increased but decreased with pH (2 - 6). Corrosion inhibition efficiency of OGHE is a function of its concentration and ability to be easily absorbed on Al surface to form thick protective films against H_2SO_4 attack. Adsorption of OGHE molecule on Al surface in 1.5 M H_2SO_4 solution agrees excellently well with Langmuir isotherm. Thermodynamic study revealed the adsorption process to be spontaneous, endothermic and physisorption in nature. Kinetic study affirmed adsorption of OGHE molecule on Al surface to obey second order reaction. Appropriate corrosion mechanisms of Al dissolution in H_2SO_4 and in the presence of OGHE were proposed. This study proved positive prospects of OGHE as effective corrosion inhibitor for Al in acidic medium.

Keywords: *Aluminium, Sulphuric acid, Oryza Glaberrima, Corrosion, Inhibition*

INTRODUCTION

It's no more new around the globe that corrosion is a deadly phenomenon [1] which could lead to loss of lives and properties. It also adversely affects the economy of developing and developed nations due to costs normally

[a] *Unit Operation and Material Science Laboratory, Chemical and Petroleum Engineering Department, Afe Babalola University, Ado-Ekiti, Ekiti State, Nigeria.*
** Corresponding author: popoolalekantaofeek@yahoo.com*

assigned to replacement of damaged materials [2]. Thus, all hands must be on desk to safe our materials (metals and alloys) from corrosion. Among these materials that is abundantly available and cut across edges of processing industries is the aluminium (Al) due to its lightness; versatility; highness in corrosion resistance, conductivity and reflectivity; non-ferromagnetic and non-pyrophoric; non-toxic; attractiveness; recyclability and easily fabricated characteristics [3]. Also, the significance of sulphuric acid in process industries cannot be ignored due to its application in cleaning, oil wet cleaning, descaling and pickling [4]. Thus, availability of Al in abundance and its aforementioned properties qualify its application in aggressive medium (such as sulphuric acid solution) which causes its corrosion over time. This prompted researchers to investigate cheap and environmental friendly corrosion inhibition approaches of Al via the use of extracts from greeners as corrosion inhibitors for aluminium in sulphuric acid solution [3, 5-15]. They are blessed with organic compounds enriched with nitrogen, phosphorus, sulphur and/or oxygen which act as agents for aluminium steel surface protection from corrosion when absorbed (physically or chemically) on its surface via π bonds, heterogeneous atoms or aromatic rings [16].

Recently, studies have investigated isotherm, kinetic and thermodynamic nature of *Dryopteris cochleata* [14], *Solanummelongena L.* [8], *Euphorbia hirta* [10], *Anthocleista djalonesis* [17], *Spondias mombin* [11], *Ocimum gratissium* [18] and *Azadirachta indica* [12] plant extracts as corrosion inhibitors for aluminium in H_2SO_4 solution. However, there were none or limited studies on isotherm, kinetic and thermodynamic characteristics of rice husk extract as corrosion inhibitor for aluminium in sulphuric acid solution. Also, most previous studies only applied Langmuir isotherm to check for data fitness of existing interaction between adsorbed molecules of inhibitors and metal surface. They rarely examined other isotherm models for comparison purpose to reveal the best fit model. Recently, *Oryza Glaberrima* husk has been shown to be very rich in silicates which contain phenolic compounds that have strong affinity to form thick films on metal surface when absorbed and thus, prevent it from corrosion under acidic attack [15, 19-20]. This study uniquely investigated isotherm, kinetic and thermodynamic studies of corrosion inhibition of aluminium in 1.5 M sulphuric acid solution using *Oryza Glaberrima* husk extract (OGHE) as corrosion inhibitor. In this study, Langmuir, Freundlich, Frumkin, Temkin and Flory-Huggins isotherm models were used to validate experimental data. Characterization of aluminium and extract was done using SEM, EDS, FTIR and AAS.

RESULTS AND DISCUSSION

Aluminium coupon and OGHE characterization

SEM

Scanning electron microscope image revealed serious corrosion attack (leading to pitting corrosion) on Al surface in 1.5 M H_2SO_4 in the absence of OGHE (Figure 1a) resulting from the formation of aluminium sulphide complexes ($[AlSO_4]^+$ and $[AlOHSO_4]$) during dissolution of Al and H_2SO_4. It was obvious that Al surface porosity increased coupled with formation of small holes. Protective film formation as a result of OGHE molecules adsorption on Al surface serves as a barrier between Al surface and H_2SO_4 and thus, prevents it from corrosion attack (Figure 1b).

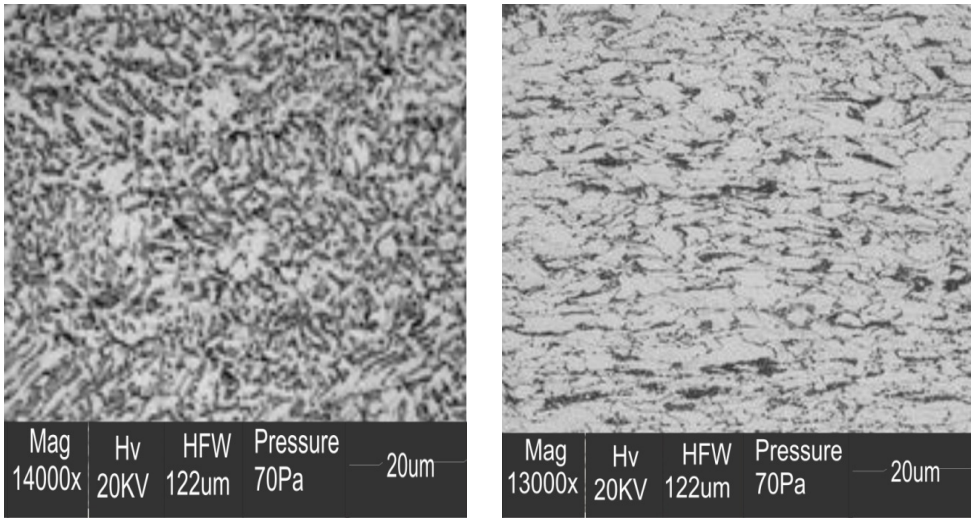

(a) (b)

Figure 1. SEM micrographs of Al surfaces (a) after immersion in 1.5 M H_2SO_4 solution in the absence of OGHE and (b) after immersion in 1.5 M H_2SO_4 solution in the presence of 1.0 g L^{-1} OGHE for 24 h at 303 K

FT-IR

Table 1 presents wavelengths and respective assignments of sharp peaks from the FT-IR analysis executed for the OGHE and corrosion products of Al in 1.5 M H_2SO_4 and 1.0 g L^{-1} OGHE. The major assignments which have high significant contributions in corrosion inhibition of Al in H_2SO_4 solution with 1.0 g L^{-1} of OGHE are peaks at: (1) 4117.84 - 3428.15 cm^{-1} attributed to

-OH stretching of phenols and alcohols. (2) 2522.20 - 2861.88 cm^{-1} resulted from N-H stretching of amine. (3) 893.7 cm^{-1} attributed to Al=S stretching resulting from covalent bond between Al and S during dissolution of Al in the corrosive medium. (4) 615.35 – 644.93 cm^{-1} attributed to Si-O stretching resulting from covalent bond between free silicon from OGHE silicate and free valent oxygen in aqueous solution. and (5) 415 cm^{-1} resulting from Al=O stretching as a result of strong electrovalent bond between dissolved Al and oxygen during its dissolution in H_2SO_4 solution in the absence of OGHE. Above all, shift in the values of peaks at different wavelengths is a strong indication of OGHE adsorption onto Al surface in 1.5 M H_2SO_4.

Table 1. Wavenumbers and assignments of FTIR sharp peaks for OGHE; and Al corrosion products in 1.5 M H_2SO_4 and 1.0 g/L OGHE

FT-IR Wavenumber (cm^{-1})		Assignments	References
OGHE	**Corrosion products of Al in 1.5 M H_2SO_4 + 1.0 g/L OGHE**		
4103.72	4117.84	-OH stretching vibration of phenols and alcohols	[21]
3428.15	3432.78	-OH stretching of phenols and alcohols	[14]
2861.88	2522.2	N-H stretching of amine	[7]
1777.38	1781.59	-C=O stretching of aliphatic ketone	[21]
1536.02	1470.08	COO^- stretching vibration	[4]
1386.20	-	NO_2 stretching vibration	[22]
-	1041.41	CO-O-CO stretching of anhydride	[7]
-	893.47	Al=S stretching	[23]
615.35	644.93	Si-O stretching	[24]
-	415	Al=O stretching	[24]

EDS

Table 2 presents the results of the energy dispersive spectroscopy analysis at certain points on the surface of Al coupon in (a) its purchased form (b) the presence of 1.5 M H_2SO_4 and (c) the presence of 1.0 g L^{-1} of OGHE with 1.5 M H_2SO_4. The following are strong evidences of Al loss to H_2SO_4 solution during dissolution in corrosive medium: (1) reduction in the weight percent of Al from 97.77 % (in its original form) to 90.04 % (in corrosive medium) (2) presence of sulphur, oxygen and hydrogen on Al surface which could be traced to corrosion attack from H_2SO_4 as these are major elements of

the acid in solution and (3) reduction in the weights of alloys of Al (except Si) during the dissolution of parent Al. The reason behind increase in the weight percent of silicon is opened for further studies. Though there was loss of Al to solution with presence of S, O and H on Al surface when 1.0 g L^{-1} of OGHE was added, the weight percentages in this regard were very minute. This proved the efficacy of OGHE to form protective films on Al surface acting as barrier between it and corrosive H_2SO_4 solution. This in return prevents the Al surface from pitting and restricts formation of small holes.

Table 2. Energy dispersive spectroscopy analysis of Al coupon in (a) purchased form (b) 1.5 M H_2SO_4 and (c) 1.5 M H_2SO_4 + 1.0 g L^{-1} OGHE

Element	Aluminium Sample (mass wt %)	Aluminium Sample in 1.5 M H_2SO_4 (mass wt %)	Aluminium Sample in 1.5 M H_2SO_4 + 1 g L^{-1} OGHE (mass wt %)
Al	97.77	90.04	97.68
S	-	3.91	0.11
O	-	2.81	0.090
H	-	1.37	0.089
Mg	1.12	0.91	1.03
Si	0.49	0.52	0.55
Mn	0.47	0.33	0.33
Fe	0.099	0.086	0.096
Zn	0.019	0.0092	0.0063
Ti	0.0096	0.0059	0.0082
Cu	0.0154	0.0044	0.0047
Cr	0.0043	0.0027	0.0036
Pb	0.0027	0.0018	0.0022

AAS

Figure 2 is the pictorial representation of the results of atomic adsorption spectroscopy analysis conducted to confirm concentration of Al^{3+} loss to H_2SO_4 solution during Al dissolution in the absence of OGHE. In contrary, Al^{3+} concentration was also checked in the presence of OGHE in H_2SO_4 to ascertain the effectiveness of OGHE as corrosion inhibitor for Al in this corrosive medium. The result revealed increase in Al^{3+} concentration in H_2SO_4 solution from 0.17 to 0.87 ppm as the exposure time increased from 24 to 120 hours. Thus, the higher the exposure period in the absence of OGHE, the higher the Al^{3+} concentration. However, reduction in Al^{3+} concentration in H_2SO_4 solution in the presence of OGHE was noticed as Al^{3+} concentration reduced

from 0.17 to 0.0096 ppm and 0.87 to 0.0696 ppm at 24 and 120 hours respectively. This affirms that OGHE is effective in minimising corrosion rate of Al in the acidic medium.

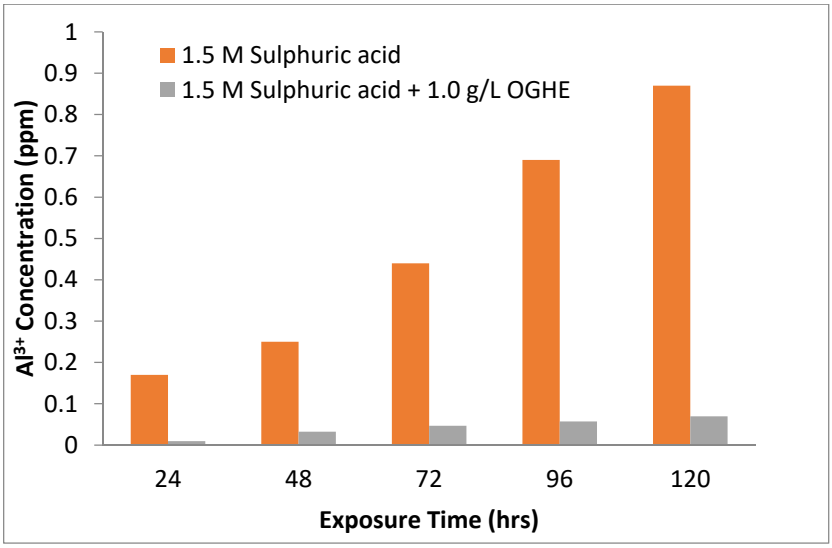

Figure 2. Al^{3+} variation after exposure period at 24 hrs interval in 1.5 M sulphuric acid solution in the absence and presence of OGHE

Effect of solution pH

The results showing pH effect (2, 4 and 6) of 1.5 M H_2SO_4 on corrosion rate of Al (Figure 3a) and inhibition efficiency of OGHE (Figure 3b) at constant temperature, exposure time and OGHE concentration of 40^oC, 24 hours and 0.6 g L^{-1} respectively have been presented. Sodium hydroxide pellets was used to vary the pH of the acidic medium. The result revealed decrease in the rate of corrosion of Al from 2.718 to 0.982 mm y^{-1} as the solution pH increases from 2 to 6 while OGHE inhibition efficiency increases from 33.48 to 64.83% in this trend. These are strong indications of high activeness of the sulphuric acid to attack the Al substrate at low pH and OGHE to protect the Al surface from acidic attack at high pH via formation of protective films. Similar trends have been presented previously [6,9].

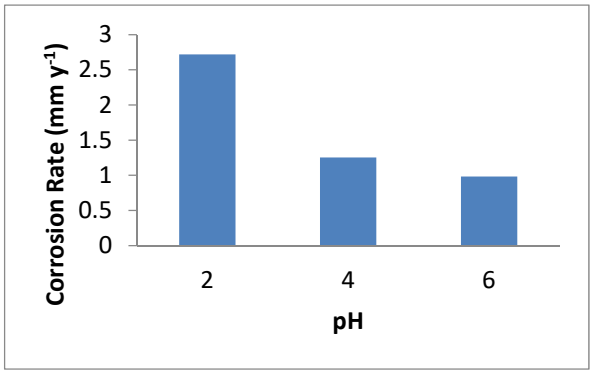

(a)

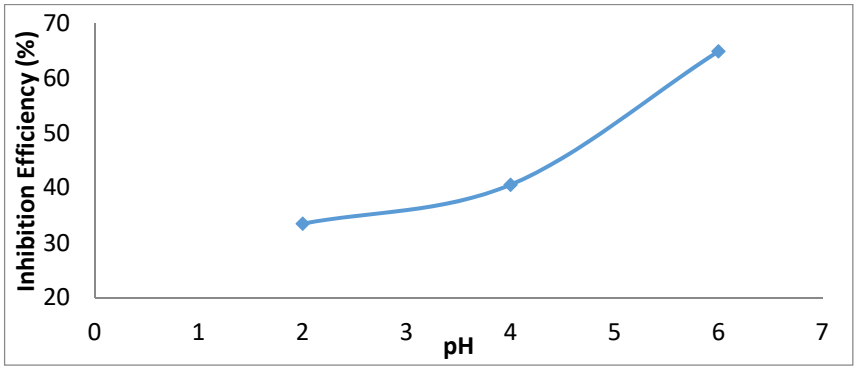

(b)

Figure 3. Effect of H_2SO_4 solution pH on (a) corrosion rate of Al and (b) inhibition efficiency of OGHE

Effect of exposure period and OGHE concentration

Figure 4 presents the results showing the effect of exposure period of Al in 1.5 M H_2SO_4 solution on the corrosion rate (Figure 4a) and inhibition efficiency of OGHE (Figure 4b) at varying exposure period of 24, 48, 72, 96 and 120 hours and OGHE concentration of 0.2, 0.4, 0.6, 0.8 and 1.0 g L^{-1}. It was observed that the corrosion rate increases as the exposure period progresses but it decreases with increase in OGHE concentration (Figure 4a). This exhibition could be linked to blockage of Al surface from H_2SO_4 attack by increase protective films formation as the concentration of OGHE increases. The corrosion rate reduced from 289.99 mm y^{-1} (blank solution) to 23.93 mm y^{-1} (in the presence of 1.0 g L^{-1} of OGHE) after exposure period of 120 hours. Similar study had presented similar result [23].

Contrary result was observed for the inhibition efficiency of OGHE used as corrosion inhibitor as its capacity to block corrosion sites on the Al reduces as the exposure period increases. However, OGHE exhibited high inhibition efficiency of 91.75% when its concentration was increased to 1.0 g L^{-1} after Al was placed in 1.5 M H_2SO_4 solution for 120 hours. This affirms the effectiveness of OGHE at high concentration as good corrosion inhibitor for Al in 1.5 M H_2SO_4 solution. Previous study presented similar trend when *Dryopteris cochleata* leaf extracts was used as green corrosion inhibitor for aluminium in 1 M H_2SO_4 solution [14].

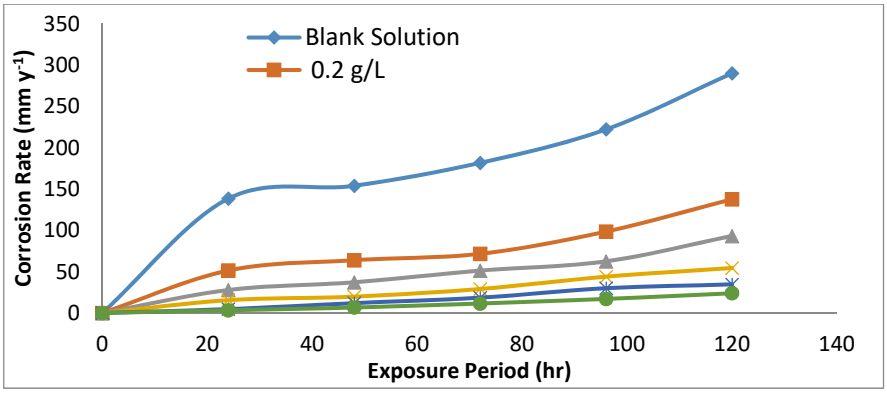

(a)

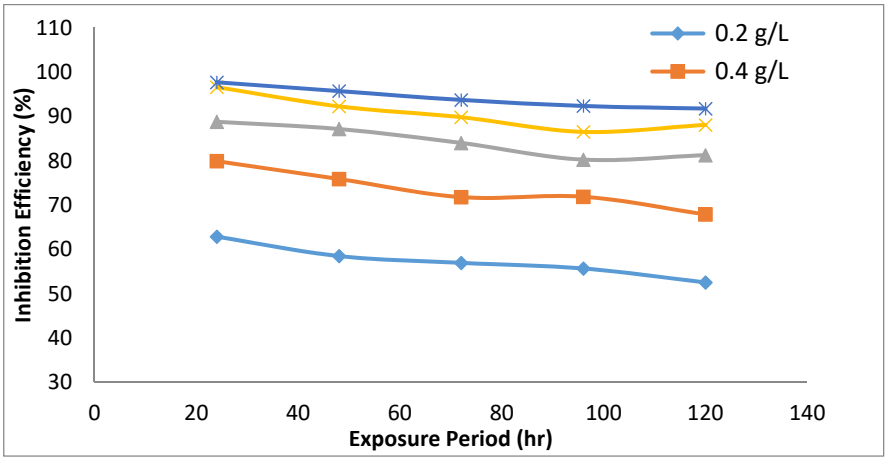

(b)

Figure 4: Effect of exposure period and OGHE concentration on (a) corrosion rate of Al and (b) inhibition efficiency of OGHE in 1.5 M H_2SO_4 solution

Temperature effects, isotherm and thermodynamic studies

The significance of studying the effects of temperature is to have thorough knowledge of adsorptive characteristics of green corrosion inhibitor molecules on metal surface when subjected to different temperature conditions [25]. Nevertheless, it's a major tool in thermodynamic and activation parameters calculation for the corrosion process. The effect of temperature on corrosion rate of Al in 1.5 M H_2SO_4 solution in the presence and absence of OGHE was examined. Also, adsorptive nature of OGHE molecules on Al surface at different temperature was investigated via inhibition efficiency measurement. Experiment was conducted at 293, 303, 313, 323 and 333K for varying OGHE concentrations of 0.2, 04, 0.6, 0.8 and 1.0 g L^{-1} while other parameters (pH = 2.0 and exposure period = 24 hours) were held constant. Increase in corrosion rate was observed in both the blank solution and presence of OGHE at different concentrations as the temperature increases (Figure 5a). Also, decrease in OGHE inhibition efficiencies was exhibited as the temperature was increased from 293 to 333 K (Figure 5b). However, the efficacy of used OGHE was displayed as its inhibition efficiency increases with increase in its concentration in H_2SO_4 solution. This affirms partial desorption of OGHE adsorbed molecules on Al surface at higher temperatures. This enhances exposure of Al surface to the corrosive medium and thus, manifested in the reduction of OGHE inhibition efficiency as solution temperature increases. However, inhibition efficiency of 88.60 % was recorded (even at high solution temperature of 333 K) when 1.0 g L^{-1} of OGHE was applied. This assures applicability of OGHE as excellent corrosion inhibitor even at relatively higher temperatures. Previous studies had presented similar results [18, 26].

Adsorption isotherm study gives insight into the nature of adsorption process showing the type of interaction existing between adsorbed molecules of green corrosion inhibitor (GCI) and metal surface which prevents its attack in aggressive media [23]. Research has shown influential factors to include: aggressive media type; chemical structures present in organic compounds of GCI; GCI molecules charge distribution; and surface charge available on metal type [5]. In this study, adsorption of OGHE molecules onto Al surface was achieved via replacement of adsorbed water molecules (H_2O_{ads}) on Al surface with OGHE molecules in aqueous phase ($OGHE_{soln}$) as written in Equation 4.

$$OGHE_{soln} + xH_2O_{ads} \longrightarrow OGHE_{ads} + xH_2O_{soln} \quad (4)$$

where $OGHE_{ads}$ stands for adsorbed OGHE molecules, H_2O_{soln} is the water molecules in solution and *x* is the number of replaced water molecules by unit molecule of adsorbed OGHE. A balanced adsorption process is then achieved when the chemical potential on both sides is the same.

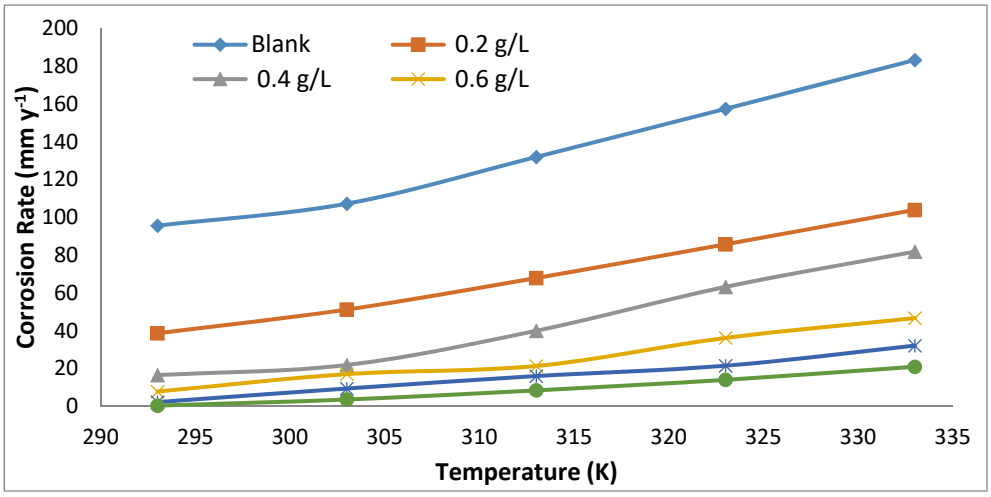

(a)

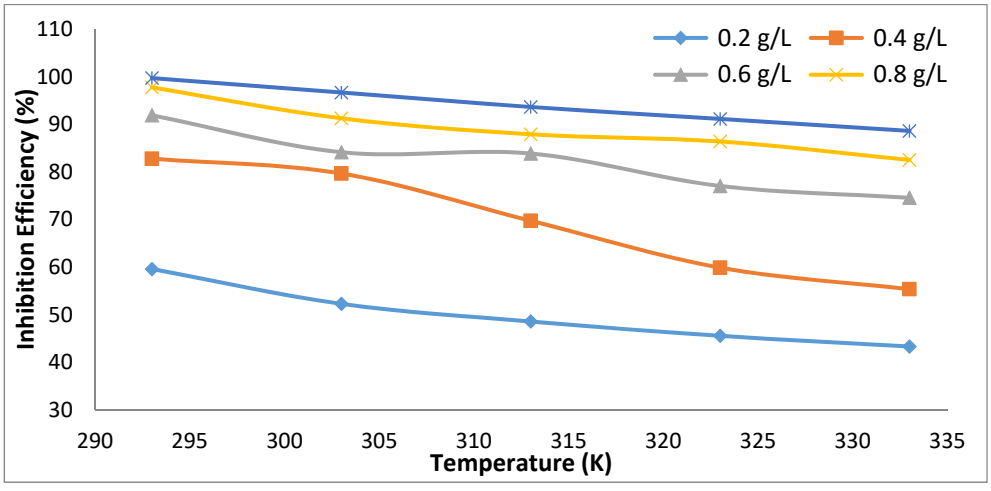

(b)

Figure 5. Effect of temperature on (a) corrosion rate of Al in H_2SO_4 solution and (b) inhibition efficiency of OGHE

In this study, linear forms of Langmuir, Freundlich, Frumkin, Temkin and Flory-Huggins stated as Equations 5-9 respectively were used to investigate nature of interaction existing between OGHE (green corrosion inhibitor) and Al surface.

$$\frac{C_{inh}}{\theta} = \frac{1}{K_{ads}} + C_{inh} \tag{5}$$

$$\log\theta = \log K_{ads} + n\log C_{inh} \qquad (0 < n < 1) \tag{6}$$

$$\log\left[C_{inh} \times \left(\frac{\theta}{1-\theta}\right)\right] = 2.303\log K_{ads} + 2\alpha\theta \tag{7}$$

$$\theta = \frac{2.303\log K_{ads}}{2a} - \frac{2.303\log C_{inh}}{2a} \tag{8}$$

$$\log\left(\frac{\theta}{C_{inh}}\right) = \log K_{ads} + x\log(1-\theta) \tag{9}$$

where C_{inh} represents OGHE concentration (g L^{-1}), K_{ads} is the adsorption equilibrium constant (g^{-1} L), θ is the surface coverage, n is a constant that measures degree of heterogeneity, α is a constant that reveals adsorbed layer nature, a is the parameter of attractiveness and x is parameter size which measures adsorbed water molecules quantity displaced by molecules of inhibitor.

Based on the result obtained (Table 3) for all plotted isotherm models (Figures 6(a)-(e)), Langmuir revealed highest R^2 value (absolutely close to unity) at all temperatures examined which substantiates it as the model that best describes the experimental data. This suggests adsorption of OGHE on Al surface assumed a mono layer adsorption (each adsorption site on solid surface is attached to one adsorbed species) [27]. Similar study also revealed Langmuir as the best isotherm model for corrosion inhibition of aluminium alloys in acidic media [28]. Also, values of K_{ads} (Langmuir) decreases as the temperature increases which revealed reduction in the inhibition efficiency of OGHE in this trend (Table 3). Value of K_{ads} is a measure of adsorptive strength of inhibitors on metal surface. The higher the values of K_{ads}, the better the adsorption and inhibition efficiency [29].

Nonetheless, parameters from other isotherms (besides Langmuir) have their significance on isotherm study of OGHE on Al in H_2SO_4 solution irrespective of their low R^2 values. The values of lateral interaction constant (α) obtained from Frumkin isotherm were all positive at investigated temperatures (Table 3) which suggests OGHE efficacy as good corrosion inhibitor for Al in aggressive media [30]. Values of attractive parameter (a) gotten from Temkin isotherm were all negative (Table 3) suggesting existence of repulsive forces between adsorbed layer of OGHE molecules on Al surface and sulphuric acid

[10]. Also, values of size parameter (x) obtained from Flory-Huggins isotherm were all positive (Table 3) which proves the bulkiness of OGHE adsorbed species [31].

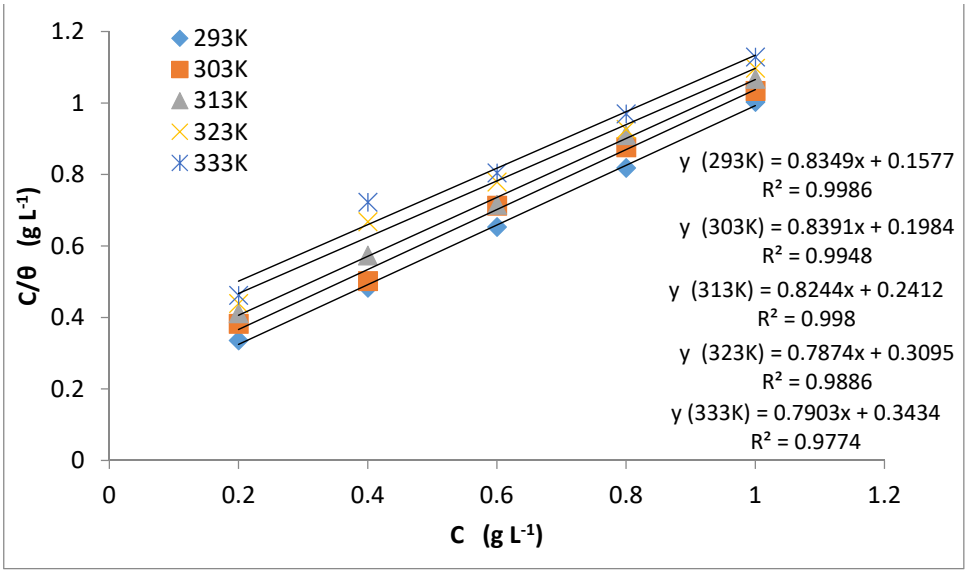

(a)

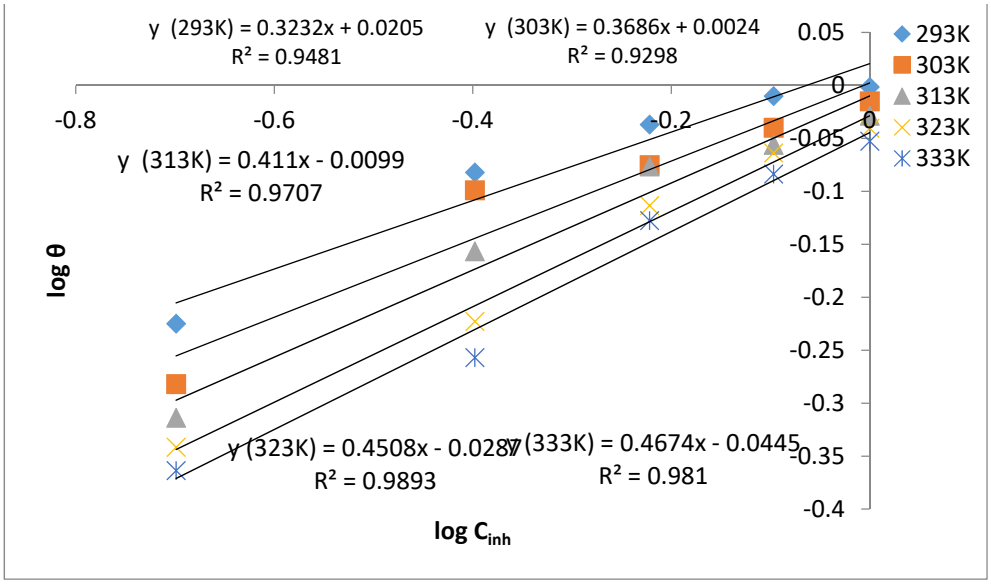

(b)

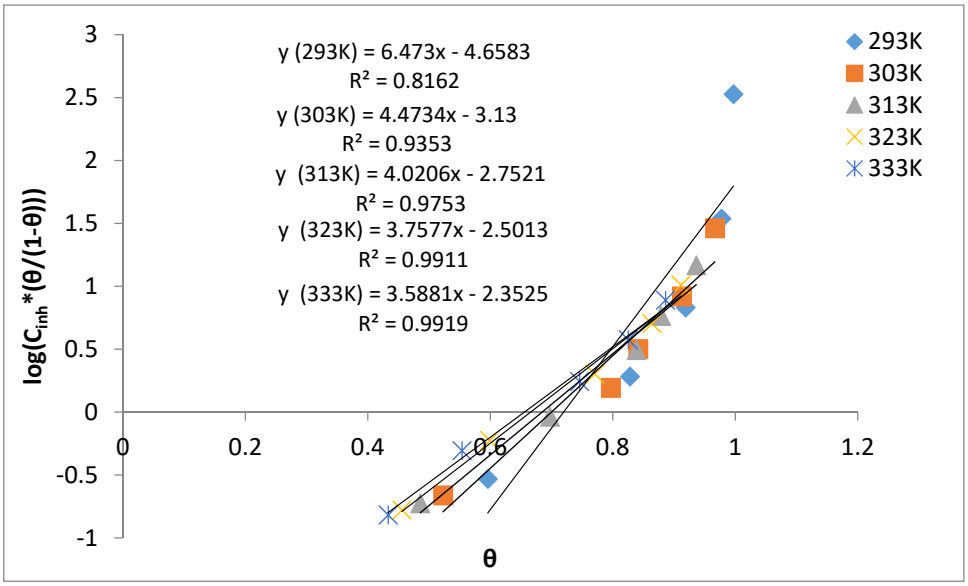
y (293K) = 6.473x - 4.6583
R² = 0.8162
y (303K) = 4.4734x - 3.13
R² = 0.9353
y (313K) = 4.0206x - 2.7521
R² = 0.9753
y (323K) = 3.7577x - 2.5013
R² = 0.9911
y (333K) = 3.5881x - 2.3525
R² = 0.9919
293K
303K
313K
323K
333K
log(C_inh *(θ/(1-θ)))
θ

(c)

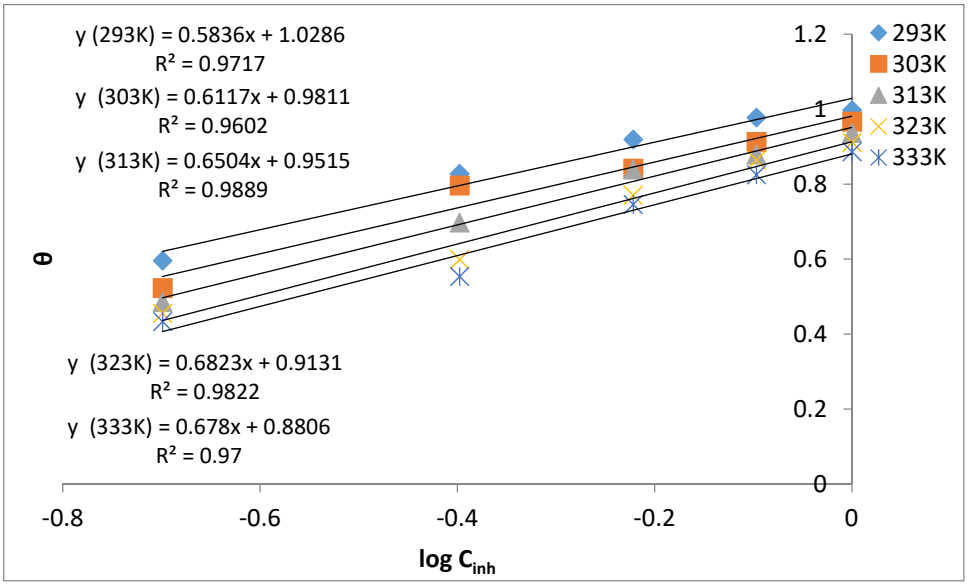
y (293K) = 0.5836x + 1.0286
R² = 0.9717
y (303K) = 0.6117x + 0.9811
R² = 0.9602
y (313K) = 0.6504x + 0.9515
R² = 0.9889
y (323K) = 0.6823x + 0.9131
R² = 0.9822
y (333K) = 0.678x + 0.8806
R² = 0.97
293K
303K
313K
323K
333K
θ
log C_inh

(d)

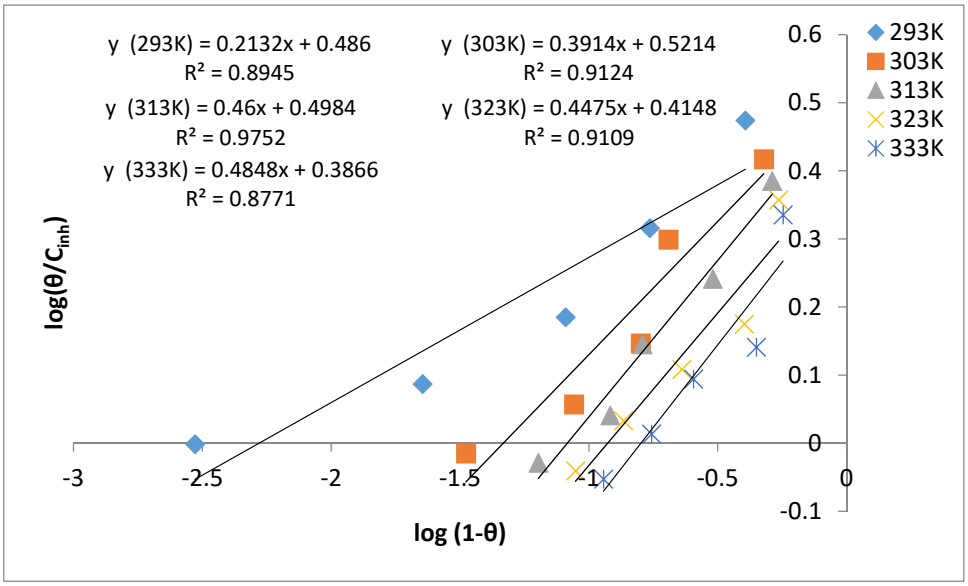

(e)

Figure 6: Isotherm study of OGHE adsorption onto Al in 1.5 M H_2SO_4 using (a) Langmuir (C_{inh}/θ vs. C_{inh}) (b) Freundlich (log θ vs. log C_{inh}) (c) Frumkin (log (C_{inh}*(θ/1-θ)) vs. θ) (d) Temkin (θ vs. log C_{inh}) and (e) Flory-Huggins (log (θ/C_{inh}) vs. log (1-θ)) isotherm models.

Table 3. Isotherm parameters of OGHE adsorption onto Al surface in 1.5 M H_2SO_4

T (K)	Langmuir		Freundlich			Frumkin			Temkin			Flory-Huggins		
	K_{ads}[a]	R^2	K_{ads}	*n*	R^2	K_{ads}	α	R^2	K_{ads}	*a*	R^2	K_{ads}	*x*	R^2
293	6.34	0.999	1.05	0.323	0.948	0.009	3.237	0.816	0.017	-1.973	0.972	3.062	0.213	0.895
303	5.04	0.995	1.01	0.369	0.930	0.044	2.237	0.935	0.025	-1.882	0.960	3.322	0.391	0.912
313	4.15	0.998	0.98	0.411	0.971	0.064	2.010	0.975	0.034	-1.770	0.989	3.151	0.460	0.975
323	3.23	0.987	0.94	0.451	0.989	0.082	1.879	0.991	0.046	-1.688	0.982	2.599	0.448	0.911
333	2.91	0.977	0.90	0.467	0.981	0.095	1.794	0.992	0.050	-1.698	0.970	2.436	0.485	0.877

[a] K_{ads}: g^{-1} L

The values of adsorption equilibrium constant (K_{ads}) obtained at different temperatures (Table 3) from the best fit isotherm (Langmuir) were used in determining thermodynamic adsorption parameters. The free energy of adsorption (ΔG^o_{ads}) was determined by solving Equation 10 at varying temperatures and K_{ads} values. The heat of adsorption (ΔH^o_{ads}) was determined from slope of a plot of $\Delta G^o_{ads}/T$ against $1/T$ using Equation 11. Gibbs-Helmholtz equation stated as Equation 12 was used to calculate the enthalpy of adsorption while Equation 13 was used to calculate the entropy of adsorption (ΔS^o_{ads}).

$$\Delta G^o_{ads} = -RTIn(55.5K_{ads}) \tag{10}$$

$$\frac{\Delta G^o_{ads}}{T} = -\frac{\Delta H^o_{ads}}{T} + \text{constant} \tag{11}$$

$$\frac{\partial \Delta G/T}{\partial T} = -\frac{\Delta H}{T^2} \tag{12}$$

$$\Delta G^o_{ads} = \Delta H^o_{ads} - T\Delta S^o_{ads} \tag{13}$$

where R = molar gas constant (8.314 $Jmol^{-1}K^{-1}$) , T = absolute temperature (K) and 55.5 = constant value denoting water concentration in solution (mol dm^{-3}).

It was observed that all the values of ΔG^o_{ads} obtained at the examined temperatures were all negative (Table 4) which suggests adsorption of OGHE on Al surface to be spontaneous with formation of stable protective film layers which protect metal surface from H_2SO_4 attack [32]. Also, values of ΔG^o_{ads} being less that -20 kJ mol^{-1} suggest existence of electrostatic attractive force of interaction (physisorption) between OGHE charged molecules and charged Al [33]. The value of ΔH^o_{ads} obtained via the linear plot of $\Delta G^o_{ads}/T$ against $1/T$ (Figure 7) was negative which signifies that the adsorption of OGHE molecules onto Al surface was exothermic in nature. Also, measured absolute value of ΔH^o_{ads} within the temperature range was less than 40 kJ mol^{-1} suggesting corrosion inhibition of Al in H_2SO_4 solution was as a result of physical adsorption of OGHE on Al surface. Nonetheless, mean positive value of ΔS^o_{ads} suggest substitution process between

adsorbed water molecules (H_2O_{ads}) on Al surface and OGHE molecules in aqueous phase ($OGHE_{soln}$) to cause rise in solvent entropy coupled with additional water desorption entropy [33].

Table 4. Thermodynamic parameters of OGHE adsorption onto Al surface in 1.5 M H_2SO_4

T (K)	K_{ads}	ΔG^o_{ads} (kJ mol^{-1})	R^2	ΔH^o_{ads} (kJ mol^{-1})	ΔS^o_{ads} (J mol^{-1} K^{-1})
293	6.34	-14.28	0.992	-16.28	97.362
303	5.04	-14.19			
313	4.15	-14.15			
323	3.23	-13.93			
333	2.91	-14.08			

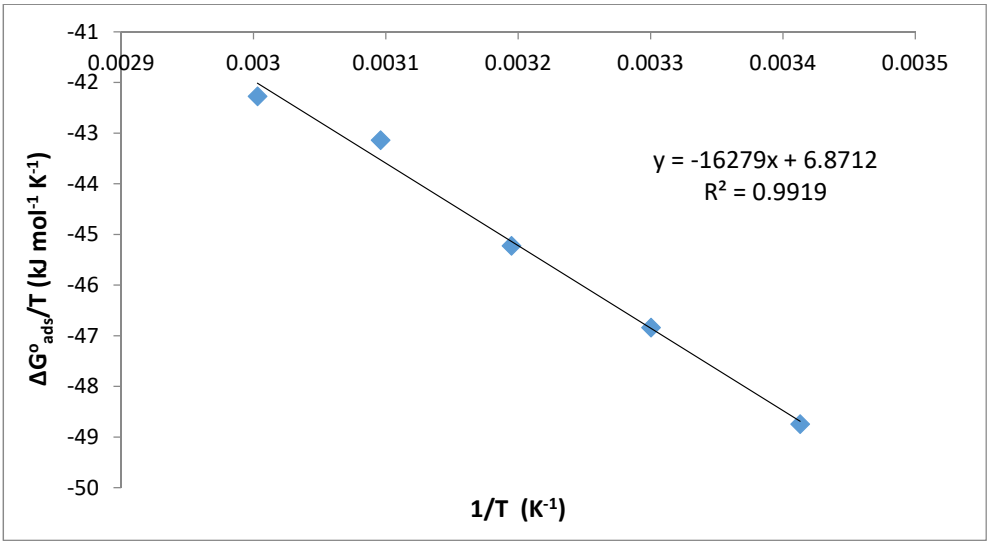

Figure 7. Plot of $\Delta G^o_{ads}/T$ vs. 1/T to determine ΔH^o_{ads} and ΔS^o_{ads} as thermodynamic parameters of OGHE adsorption onto Al surface in 1.5 M H_2SO_4

Kinetics and order of reaction

Analysis of kinetic data of corrosion reaction is imperative due to its heterogeneous nature (cathodic and anodic reaction pathways). To achieve this, determination of rate constants and half life parameters are required to identify the order of reaction. Table 5 presents the results of half life and rate constants obtained from first order plot (*ln (W_1 - W_2)* vs. *t*) presented as Figure 8a

and second order plot (t/W_2 vs. t) presented as Figure 8b via Equations 14 - 16 respectively [15] at varying OGHE concentrations (0.2 – 1.0 g/L), time (24 - 120 hours) and constant temperature of 313 K in 1.5 M H_2SO_4 solution.

$$t_{1/2} = \frac{0.693}{k} \tag{14}$$

$$\ln(W_1 - W_2) = -kt + \ln W_1 \tag{15}$$

$$\frac{t}{W_2} = \frac{1}{k_2 W_1^2} + \frac{t}{W_1} \tag{16}$$

where W_1 = initial weight of the metal (g), W_2 = final weight of the metal (g), k = rate constant, t = exposure time (h) and $t_{1/2}$ = half life.

The result (Table 5) revealed increase in rate constants for both order of reactions as the inhibitor concentration increases with decrease in corrosion rate. This substantiates the effectiveness of OGHE as corrosion inhibitor for Al in H_2SO_4. Also, the half-life decreases as the OGHE concentration increases which indicates decrease in the time required for Al to corrode to half of its initial weight resulting from its protection by OGHE extract via adsorption. Approximately unity values were obtained for R^2 of proposed second order linear model (Table 5) which supports it as the model that best describes the order of the corrosion reaction of Al in H_2SO_4 in the presence of OGHE. However, previous studies rarely considered this proposed second order linear model. They usually present first order linear model (Equation 15) as the best model for R^2 values between 0.930 and 0.980 [31, 34-35]. In this study, similar result was also revealed for the linear first order kinetic model as R^2 ranges between 0.930 and 0.992.

Results revealed by both first and second order kinetic linear models was substantiated via application of rate order reaction equation (Equation 17) to determine order of reaction (n). The linearized form of the equation is presented as Equation 18. The experiment was conducted for 120 hrs at 24 hrs time interval to obtain a linear plot of $ln\ r_c$ vs. $ln\ C_{inh}$ (Figure 9) such that the slope of each plot is the order of reaction. The result revealed all values of n to be greater than 1 with minimum and maximum values being 1.0898 and 1.7561 (Table 6) respectively. The order of reaction can be approximated to be 2 which affirms the result earlier presented.

$$r_c = kC_{inh}^n \tag{17}$$

$$\ln r_c = \ln k + n \ln C_{inh} \tag{18}$$

where r_c is the rate of corrosion (mm y^{-1}), k is the reaction constant, n is the order of reaction and C_{inh} is concentration of OGHE (g L^{-1}).

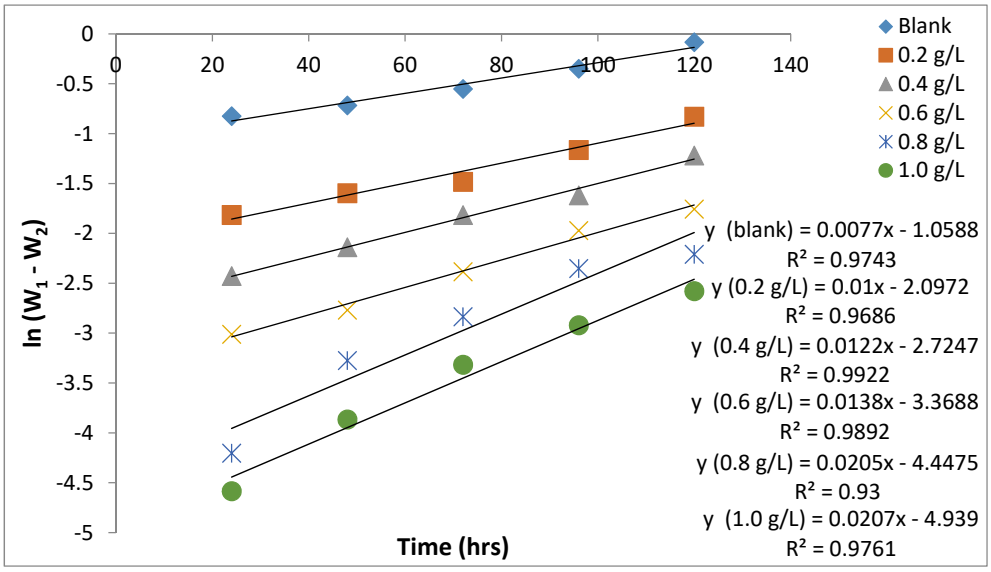

(a)

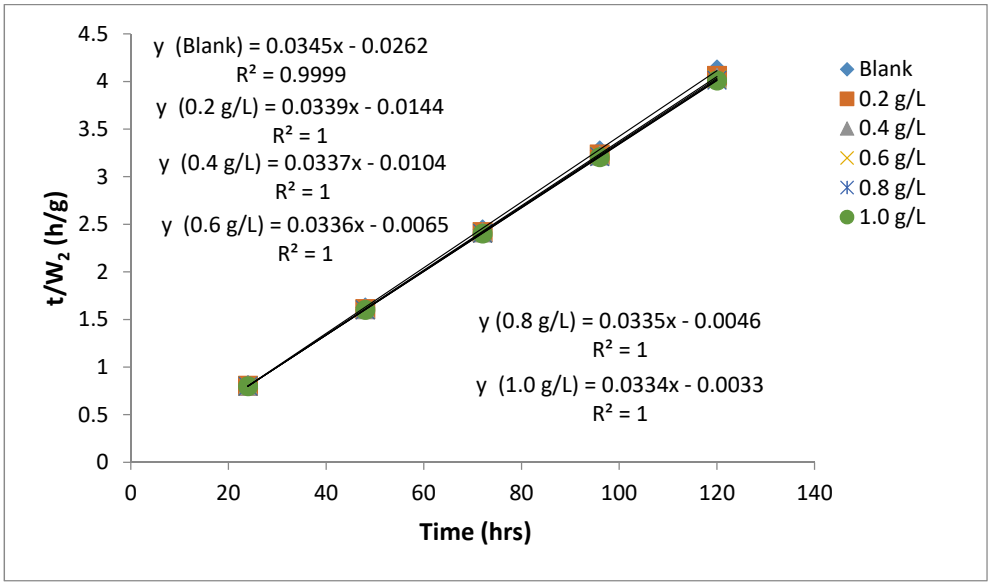

(b)

Figure 8. Kinetic study of OGHE adsorption onto Al surface in 1.5 M H_2SO_4 using (a) first order and (b) second order linear models

Table 5. Kinetic parameters of OGHE adsorption onto Al surface in 1.5 M H_2SO_4

System	First order			Second order		
	$k_1 \times 10^{-2}$ (hr^{-1})	$t_{1/2}$ (hr)	R^2	$k_2 \times 10^{-2}$ ($g^{-1}hr^{-1}$)	$t_{1/2}$ (hr)	R^2
Blank	0.77	90.00	0.974	4.54	15.25	0.999
0.2 g/L	1.01	69.30	0.969	7.98	8.68	1.000
0.4 g/L	1.22	56.80	0.992	10.92	6.35	1.000
0.6 g/L	1.38	50.22	0.989	17.37	3.99	1.000
0.8 g/L	2.05	33.80	0.930	24.40	2.84	1.000
1.0 g/L	2.07	33.48	0.976	33.80	2.05	1.000

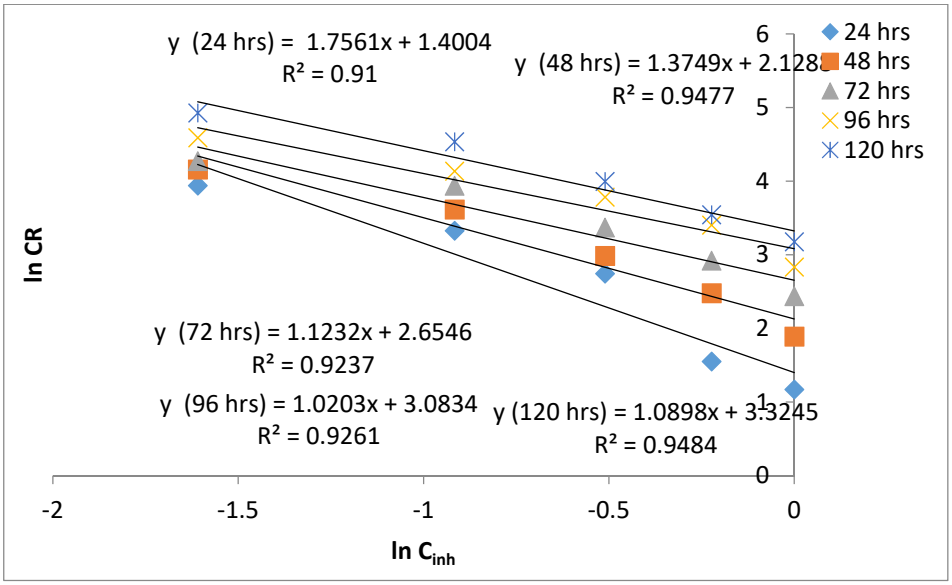

Figure 9. Plot of ln CR against ln C_{inh} to determine reaction order for OGHE adsorption onto Al surface in 1.5 M H_2SO_4

Table 6. Kinetic parameters of OGHE adsorption onto Al surface in 1.5 M H_2SO_4

Time (hrs)	*n*	R^2
24	1.7561	0.910
48	1.3749	0.948
72	1.1232	0.924
96	1.0203	0.926
120	1.0898	0.948

Corrosion inhibition mechanism

In the absence of OGHE, dissociation of H_2SO_4 and dissolution of Al (Equations 19-22) occur in solution to form 2 moles of H^+, 1 mole of SO_4^{2-}, 1 mole of Al^{3+} and 1 mole of $[AlOH]^{2+}$ ions. The sulphide ion is then adsorbed on Al surface to form aluminium sulphide complexes $[AlSO_4]^+$ and $[AlOHSO_4]$ with Al^{3+} and $[AlOH]^{2+}$ respectively in the anodic reaction. These complexes are the main soluble corroded Al form which makes its surface to corrode easily in H_2SO_4 solution in the absence of OGHE. In the cathodic reaction, 2 moles of H^+ picked up the released electron in the anodic reaction to produce chemisorbed hydrogen. The chemisorbed hydrogen then combines with each other to form H_2 gas molecule which escapes from the Al surface. The main controlling steps in the Al dissolution are the complexes formation reactions presented as Equations 23-24.

H_2SO_4 dissociation: $H_2SO_{4(aq)} \rightleftharpoons 2H^+ + SO_4^{2-}$ (19)

Al dissolution: $Al_{(s)} + H_2O \rightleftharpoons AlOH_{ads} + H^+ + e^-$ (20)

$AlOH_{ads} + 5H_2O + H^+ \rightleftharpoons Al^{3+} + 6H_2O + 2e^-$ (21)

$Al^{3+} + H_2O \rightleftharpoons [AlOH]^{2+} + H^+$ (22)

Complexes formation: $Al^{3+} + SO_4^{2-} \rightleftharpoons [AlSO_4]^+$ (23)

$[AlOH]^{2+} + SO_4^{2-} \rightleftharpoons [AlOHSO_4]$ (24)

In the presence of OGHE, corrosion inhibition of Al surface in H_2SO_4 is enhanced by:

(1) formation of thin film protective coatings resulting from adsorption of anionic OGHE on positive sites formed on Al surface due to electron liberation during the anodic reactions (Equations 20-21). The thin film acts as a barrier between Al surface and H_2SO_4 and thus prevents loss of Al atoms into the acidic solution which in return limits the corrosion rate.

(2) replacement of water molecules present in solution by adsorbed soluble OGHE molecules on Al surface which alters kinetics of Al dissolution (Equation 4).

(3) presence of functional hydroxyl groups (revealed by FTIR) in the phenolic compounds of γ-oryzanols, α-tocopherol and γ-tocopherol (Figure 10) which are major constituents of OGHE molecules [36-38]. These –OH groups bridge the gap between OGHE molecules and Al surface and thus minimises corrosion rate.

(4) presence of valent heteroatom (oxygen) attached directly to aromatic rings of α- and γ-tocopherol (Figures 10(b-c)) enhances donor–acceptor surface complexes formation between OGHE p-electrons and Al vacant d-orbital. This alters the electrochemical characteristics of the system and thus, leads to reduction in corrosion.

(5) extended size and nature of γ-oryzanols, α-tocopherol and γ-tocopherol compounds present as OGHE molecules which cover large areas on the Al surface and thus inhibit its corrosion.

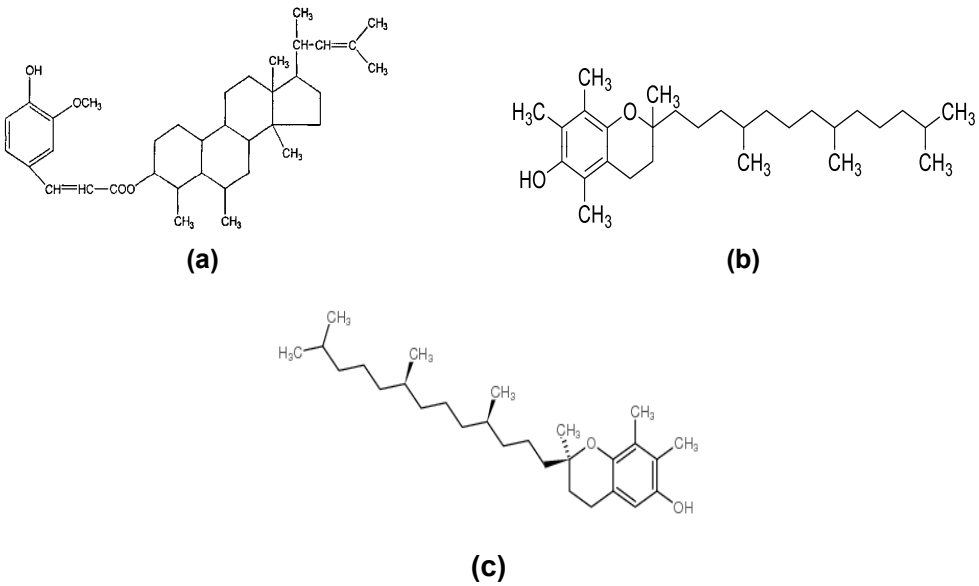

Figure 10: Phenolic compounds of (a) γ-oryzanols
(b) α-tocopherol and (c) γ-tocopherol present in OGHE

CONCLUSIONS

Experimental works executed in this study revealed that Al has corrosion resistance attributes in H_2SO_4 solution in the presence of OGHE. Formation of pitting and small holes on Al surface in H_2SO_4 solution was revealed by SEM. Presence of –OH (attached to the phenolic rings of γ-oryzanols, α-tocopherol and γ-tocopherol) and –NH was revealed by FTIR. Attachment of sulphur, oxygen and hydrogen on Al surface in aqueous H_2SO_4 was shown by EDS. Reduction in concentration of Al^{3+} loss in acidic medium in the presence of OGHE was revealed by AAS. Corrosion rate of Al increased in H_2SO_4 solution as exposure period (24 - 120 hrs) and temperature

(293 - 333K) were increased but decreased with pH (2 - 6). Corrosion inhibition efficiency of OGHE primarily depends on its concentration and adsorptive capability on Al surface via formation of thick protective films. Adsorption of OGHE molecule on Al surface in 1.5 M H_2SO_4 solution agrees perfectly with Langmuir isotherm. Thermodynamic study revealed adsorption of OGHE molecule on Al surface to be spontaneous, endothermic and physisorption in nature. Kinetic study affirmed adsorption of OGHE molecule on Al surface to follow second order reaction. Corrosion mechanism was enhanced by Al dissolution in H_2SO_4 solution and presence of –OH group attached to phenolic compounds of γ-oryzanols, α-tocopherol and γ-tocopherol present in OGHE.

EXPERIMENTAL

Materials

Table 7 presents the chemical composition of commercial aluminium used for this study supplied by Alok Hefsibah Global Trust Limited. Ethanol, acetone, grades of silicon carbide paper and sulphuric acid (*all of analytical grades*) were supplied by Top-Jay Scientific. *Oryza Glaberrima* husk, left as remnant, was obtained from Bodija International Market, Oyo State, Nigeria.

Table 7. Chemical Composition of Aluminium Used

Element	Al	Mg	Si	Mn	Fe	Zn	Ti	Cu	Cr	Pb
(%)	97.82	1.06	0.57	0.41	0.11	0.0093	0.0082	0.0061	0.0039	0.0025

Aluminium coupon preparation

Grades of silicon carbide paper were used to polish the aluminium to remove dirts. Polished aluminium was then cut into coupons of same dimension (6×4×0.4 cm) and exposed surface area (24 cm^2) with aid of a digital vernier calliper. Acetone was used to degrease the aluminium coupons while distilled water was used to thoroughly rinse them. Samples were dried and kept in desiccator for subsequent weight loss experiment.

Extract and corrosion inhibitor preparation

Clean water was used to thoroughly wash the *Oryza Glaberrima* husk to remove unwanted dirt after which it was dried in an oven for 24 hours at 120^{o}C. Mechanical grinder was used for the dried *Oryza Glaberrima* husk

and was later sieved to obtain fine particles of < 63 µm. The particles were kept in clean polythene bags and sealed to prevent further moisture contamination. Soxhlet extraction process was adopted to get extract from particles at room temperature (28 ± 3 °C) using analytical grade ethanol. The filtrate obtained (which stands as the extract used as corrosion inhibitor) was later subjected to evaporation to remove excess ethanol and then stocked for experiment. Different concentrations of *Oryza Glaberrima* husk extract (OGHE) (0.2, 0.4, 0.6, 0.8 and 1.0 g L^{-1}) were prepared and used as corrosion inhibitor for Al in 1.5 M H_2SO_4 solution.

Weight loss measurement

Aluminium coupons were tested in sulphuric acid using weight loss measurement. Weights of aluminium coupons were checked before and after immersion in 1.5 M H_2SO_4 solution in the presence and absence of OGHE. After the immersion time is elapsed, coupons were removed from acidic solution and then washed with distilled water and acetone. Specimens were dried using hot air and allowed to cool for 10 minutes. Equations 1-3 were used to calculate the corrosion rate, inhibition efficiency and surface coverage respectively using weight loss values after each experiment via digital weighing balance.

$$CR\ (mm/y) = \frac{87,500W}{A\rho t} \tag{1}$$

$$I.E.\% = \left(1 - \frac{CR_{inh}}{CR_{blank}}\right) \times 100 \tag{2}$$

$$\theta = \left(1 - \frac{CR_{inh}}{CR_{blank}}\right) \tag{3}$$

where CR = corrosion rate (mm y^{-1}), W = weight loss (g), A = coupon area (cm^2), ρ = density (g cm^{-3}), t = immersion time (hr), *I.E.%* = inhibition efficiency, CR_{inh} = corrosion rate in the presence of inhibitor and CR_{blank} = corrosion rate in the absence of inhibitor, θ = surface coverage.

Extract and coupon characterization

FTIR analysis

OGHE and corrosion products of aluminium in 1.5 M H_2SO_4 in the presence of OGHE were characterized by FTIR within wavelength of 400 - 4000 cm^{-1} via Nicolet iS10 Fourier transform infra-red spectrophotometer.

Scanning electron microscopy/energy dispersive spectroscopy

SEM/EDX-JEOL-JSM 7600F scanning electron microscope was used to examine the surface morphology of aluminium coupon in the presence and absence of OGHE. The energy dispersive spectroscopy (EDS) analysis was executed via attached accessories of scanning electron microscope.

Atomic absorption spectroscopy

AAS Buck Scientific 210 VGP atomic absorption spectrometer was used to check Al^{3+} concentration in H_2SO_4 solution after weight loss measurement.

REFERENCES

[1] D. Miller, *Mater Perform*, **1990**, *29*, 10–11.
[2] K.R. Trethewey, P.R. Roberge, *British Corro J*, **1995**, *30*, 192–197.
[3] S.K. Sharma, P. Anjali, O.I. Bassey, *J. Anal. Sci. Technol*., **2015**, *6*, 26-35.
[4] A.M. Abdel-Gaber, B.A. Abd-El-Nabey, M. Saadawy, *Corrosion Sci.*, **2009**, *51(5)* 1038-1042.
[5] A. Yurt, S. Ulutaas, H. Dal, *Appl. Sur. Sci*., **2006**, 253, 919-925.
[6] I.B. Obot, N.O. Egbedi, S.A. Umoren, *Int. J. Electrochem. Sci.*, **2009**, *4*, 863–877.
[7] A.S. Fouda, A.A. Al-Sarawy, F.S. Ahmed, H.M. El-Abbasy, *Corros. Sci*., **2009**, *51*, 485-492.
[8] M.M. Ihebrodike, A.U. Anthony, B.O. Kelechukwu, G.A. Alozie, *Afr. J. Pure Appl. Chem*., **2010**, *4*, 158-165.
[9] Q. Zhang, Z. Gao, F. Xu, X. Zou, *Colloids Surf. A Physicochem. Eng. Aspects*, **2011**, *380*, 191–200.
[10] L. Nnanna, I. Anozie, A. Avoaja, C. Akoma, E. Eti, *Afr. J. Pure Appl. Chem*., **2011**, *5*, 265-271.
[11] N.O. Obi-Egbedi, I.B. Obot, S.A. Umoren, *Arab. J. Chem*., **2012**, *5(3)*, 361–373.
[12] K.S. Sanjay, P. Anjali, I.B. Obot, *J. Anal. Sci. Technol.*, **2015**, *6*, 26-33.
[13] M. Abdallah, B.A. Al-Jahdaly, *Int. J. Electrochem. Sci.*, **2015**, *10*, 9808–9823.
[14] R.S. Nathiya, R. Vairamuthu, *Egypt. J. Petroleum*, **2017**, *26*, 313-323.
[15] L.T. Popoola, *Corros Rev,* **2019**, *37(2)*, 71-102.
[16] M. Finsgar, J. Jackson, *Corros. Sci*., **2014**, *86*, 17-41.
[17] O.O. Adeyemi, O.O. Olubomehin, *Pacific J. Sci. Technol*., **2010**, *11*, 455-462.
[18] D.I. Udunwa, O.D. Onukwuli, M. Omotioma, *Der Pharma Chemica*, **2017***, 9,* 19, 48–59.
[19] N. Mohamad, N.K. Othman, A. Jalar, *AIP Conference Proceedings*, Faculty of Science and Technology Post-Graduate Colloquium, Selangor, Malaysia, **2013**, *1571*, 136-140.
[20] M.H. Mahross, A.H. Naggar, T.A.S. Elnasr, M. Abdel-Hakim M, *Chem Adv Mater*, **2016**, *1*, 6-16.
[21] M. Grube, J.G. Lin, P.H. Lee, S. Kokorevicha, *Afr. J. Geo-chem*., **2006**, *130,* 324–333.

[22] J. Majedova, *Spectroscopy*, **2003**, *32,* 1–10.
[23] A.Y. Musa, A.A. Khadom, A.H. Kadhum, A.B. Mohamad, M.S. Takriff, *Res. Chem. Intermed*., **2012**, *38*, 91-103.
[24] H.B. Stuart, "Infrared Spectroscopy, Fundamentals and Applications", **2004**, John Wiley Sons Ltd.
[25] A. Singh, I. Ahamad, D.K Yadav, V.K. Singh, M.A. Quraishi, *Chem. Eng. Commun*., **2012**, *199*, 1, 63–77.
[26] A.J. Aldykewicz, H.S. Isaacs, A.J. Davenport, *J. Electrochem. Soc*., **1995**, *142*, 3342-3350.
[27] Q.B. Zhang, Y.X. Hua, *Electrochem. Acta*., **2009***, 54*, 1881-1887.
[28] R.M. Hassan, I.A. Zaafarany, *Materials*, **2013**, *6*, 2436-2451.
[29] R. Solmaz, *Corros. Sci*., **2014**, *79*, 169–176.
[30] V.C. Anadebe, O.D. Onukwuli, M. Omotioma, N.A. Okafor, *S. Afr. J. Chem*., **2018**, *71*, 51–61.
[31] G.A. Ijuo, H.F. Chahul, I.S. Eneji, *J. Adv. Electrochem*., **2016**, *2(3),* 107–112.
[32] H. Keleş, M. Keleş, I. Dehri, O. Serindağ, *Colloids Surf. A Physicochem. Eng. Asp*., **2008**, *320*, 138–145.
[33] M. Abdallah, M.A. Hegazy, M. Alfakeerd, H. Ahmeda, *Green Chem. Lett. Rev.*, **2018**, *11(4),* 457–468.
[34] A.O. James, N.C. Oforka, O.K Abiola, *Bull. Electrochem.*, **2006**, *22*, 111-116.
[35] O.O Fadare, A.E. Okoronkwo, E.F. Olasehinde, *African J. Pure Appl. Chem.*, **2016**, *10(1),* 8–22.
[36] A. Moongngarm, N. Daomukda, S. Khumpika, *APCBEE Procedia*, **2012,** *2*, 73–79.
[37] S.H. Huang, L.T. Ng, *J. Agric. Food Chem.,* **2011**, 59(20), 11150–11159.
[38] S. Yu, Z.T. Nehus, T.M. Badger, N. Fang, *J. Agric. Food Chem,* **2007**, *55(18),* 7308–7313.